An Alternative Domain Near the ATP Binding Pocket of *Drosophila* Myosin Affects Muscle Fiber Kinetics

Douglas M. Swank,* Joan Braddock,[†] Waylon Brown,[†] Heather Lesage,[†] Sanford I. Bernstein,[‡] and David W. Maughan[†]

*Department of Biology and Center for Biotechnology, Rensselaer Polytechnic Institute, Troy, New York; [†]Department of Molecular Physiology and Biophysics, University of Vermont, Burlington, Vermont; and [‡]Biology Department and Molecular Biology Institute, San Diego State University, San Diego, California

ABSTRACT   We examined the importance of alternative versions of a region near the ATP binding site of *Drosophila* myosin heavy chain for muscle mechanical properties. Previously, we exchanged two versions of this region (encoded by alternative exon 7s) between the indirect flight muscle myosin isoform (IFI) and an embryonic myosin isoform (EMB) and found, surprisingly, that in vitro solution actin-activated ATPase rates were increased (higher V_{max}) by both exon exchanges. Here we examined the effect of increased ATPase rate on indirect flight muscle (IFM) fiber mechanics and *Drosophila* locomotion. IFM expressing EMB with the exon 7a domain replaced by the IFM specific exon 7d domain (EMB-7d) exhibited 3.2-fold greater maximum oscillatory power (P_{max}) and 1.5-fold greater optimal frequency of power generation (f_{max}) versus fibers expressing EMB. In contrast, IFM expressing IFI with the exon 7d region replaced by the EMB exon 7a region (IFI-7a), showed no change in P_{max}, f_{max}, step response, or isometric muscle properties compared to native IFI fibers. A slight decrement in IFI-7a flight ability was observed, suggesting a negative influence of the increased ATPase rate on *Drosophila* locomotion, perhaps due to energy supply constraints. Our results show that exon 7 plays a substantial role in establishing fiber speed and flight performance, and that the limiting step that sets ATPase rate in *Drosophila* myosin has little to no direct influence in setting f_{max} for fast muscle fiber types.

INTRODUCTION

The functional diversity of striated muscle is specified by myofibrillar protein isoforms that enable specialized muscle fiber types to perform different locomotory actions (1,2). The isoforms of the molecular motor myosin are generally regarded as the primary determinants of muscle mechanical parameters, including force, velocity, and oscillatory work and power output. By expressing an embryonic isoform (EMB) myosin heavy chain (MHC) in *Drosophila* indirect flight muscle (IFM), we previously showed that myosin isoforms dictate fiber kinetics in these oscillatory power-generating muscles (3). Substituting EMB for the native indirect flight muscle isoform (IFI) transformed the IFM from a high-power-generating muscle that performs optimally at high oscillation frequencies (130–150 Hz) to one that produces less power and functions best at low oscillation frequencies (~20 Hz) (4). The fiber studies correlate with molecular studies of the myosin isoforms since IFI has a ninefold faster actin velocity and a twofold higher ATPase activity than EMB (5).

Sequence comparisons and in vitro functional studies at the molecular level suggest that specific structural domains of MHC modulate myosin functional properties (6,7). However, the importance of these domains in setting muscle mechanical properties has only recently been directly tested in organized muscle systems (4,8,9). *Drosophila's* mechanism of MHC isoform expression makes it especially valuable for structure/function studies. A diverse array of MHC isoforms is generated through alternative splicing of mRNA transcripts from the single copy *Mhc* gene (10–12). Fifteen isoforms have been identified to date, expressed in a wide variety of fiber types including the extremely fast IFM and the super-contractile embryonic body wall muscles (13). There are five sets of alternatively spliced exons in *Mhc*, four of which are in the S-1 head region, and a C-terminal exon, 18, that is either included or excluded. We have been systematically examining the importance of the individual alternative exon regions for defining functional properties of *Drosophila* myosin. By mapping the location of the alternative domains on the chicken skeletal S-1 structure, we identified regions of the molecule that set specific properties of *Drosophila* myosin (14). We are currently exchanging alternative exon versions between the IFI and EMB, which differ at all four variable regions of the S-1 motor domain (Fig. 1).

The region encoded by exon 7 may have a major influence on myosin and muscle fiber properties given its location near the entrance to the active site (residues 301–335 of chicken skeletal MHC) (Fig. 1). There are four alternative choices for exon 7. The IFI and EMB versions differ in 14 of 35 amino acids, of which eight are nonconserved substitutions (14). The IFI version, encoded by exon 7d, is expressed only in adult muscles, including the very fast IFM, the tergal depressor of the trochanter (the jump muscle), and direct flight muscle number 51. The EMB version, encoded by exon 7a,
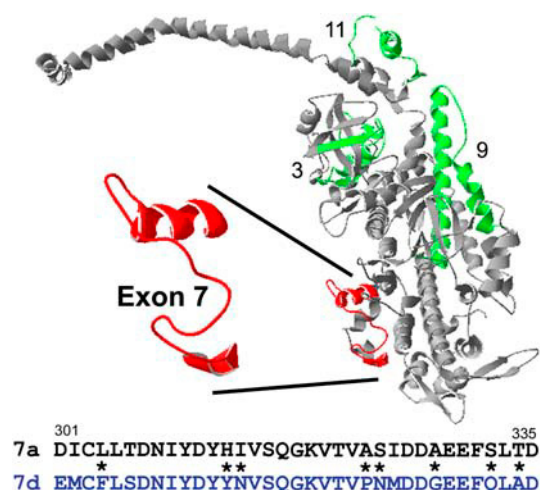
FIGURE 1   Location and alternative sequence choices for the exon 7 region. The exon 7 region (*red*) and the three other variable regions (3, 9, and 11) encoded by *Drosophila* alternative exons (*green*) are mapped onto the chicken myosin S1 structure (*gray*). The exon 7 region is part of one lip of the nucleotide entry/exit site (14). The long α-helix that binds the light chains and constitutes the lever arm is across the top of the figure and the actin binding sites are at the bottom right. The EMB (7a) and IFI (7d) amino acid sequence versions of the exon 7 region are shown below the molecular structure. Asterisks signify nonconserved substitutions.

is expressed in all embryonic body wall muscle, visceral muscle, and embryonic cardioblasts, but not in the pharyngeal muscle. Exon 7a is expressed in only one adult muscle, direct flight muscle number 52 (13,15).

Previously, we exchanged the exon 7 region between IFI and EMB myosins (16). This created two myosin chimeras referred to as IFI-7a (IFI with the EMB version of exon 7, 7a) and EMB-7d (EMB with the IFI version of exon 7, 7d). In solution, both exon 7 chimeras showed elevated myosin and actomyosin ATPase rates compared to their parent isoforms. Surprisingly, neither exon 7 chimera altered actin sliding velocity in the in vitro motility assay. Based on previous studies of myosin in other species, the elevated ATPase rates suggest that the exon 7 region influences steps of the cross-bridge cycle associated with myosin attachment to actin, i.e., the transition from weakly to strongly bound states. The unaltered velocities suggest that this region has little or no effect on myosin detachment kinetics, as detachment kinetics are thought to set in vitro motility velocity.

To further investigate the significance of the exon-7-encoded domain and its specific influence on muscle fiber properties, we examined the mechanical performance of skinned IFM fibers expressing the exon 7 chimeric MHC isoforms. We found that exchanging the IFI specific exon 7 region into EMB (EMB-7d) increased maximum oscillatory power generation (P_{max}) 3.2-fold and the optimal frequency of power generation (f_{max}) 1.5-fold compared to fibers expressing EMB. Thus, the exon 7 region accounts for a portion of the sevenfold difference in frequency of maximum oscillatory power between IFI and EMB fibers. Comparing our fiber data

with solution actomyosin ATPase studies of the exon 7 chimeras (16), we found that an increase in EMB ATPase rate correlated with an increase in EMB fiber kinetics (f_{max}), but that an increase in IFI ATPase did not correlate with IFI fiber kinetics, which remained unaltered by the exon exchange. This suggests that the actomyosin ATPase rate-limiting step has little or no direct influence on oscillatory work production kinetics of very fast *Drosophila* muscle.

METHODS

Transgenic lines

Creation of the EMB transgenic line is described in Wells et al. (3), and construction of lines expressing the exon 7 chimeras is described in Miller et al. (16). Reverse transcriptase-polymerase chain reaction and sodium dodecyl sulfate polyacrylamide gel electrophoresis confirmed that all transgenes properly expressed the expected protein (16).

To control for the possibility that the transgenes inserted into a gene that affects IFM function, we tested multiple lines generated from independent insertion events. For EMB-7d, we mechanically evaluated a second line, EMB-7d line M23C, and observed statistically identical results (see Tables 2 and 3). Because two independently generated IFI-7a lines (IFI-7a line 37A and IFI-7a line 86A) had identical flight ability and wing-beat frequencies (Table 1), we carried out mechanical evaluations on only one IFI-7a line. We have previously shown that two IFI control lines give identical mechanical results (4,9) and that two EMB control lines are mechanically identical (9). The IFI and EMB control data for this study were all generated from new experiments on these previously tested lines, rather than relying on measurements from earlier studies.

Mechanics protocol

Mechanical evaluation of fibers was performed as described in Swank et al. (9). Briefly, a single dorsolongitudinal IFM fiber was split lengthwise, producing a preparation $\sim$100 μm in diameter and $\sim$0.6 mm in length. Fibers were chemically demembranated (skinned) in a relaxing solution (5 mM MgATP, 15 mM creatine phosphate, 240 units/ml creatine phosphokinase, 1 mM free Mg^{2+}, 5 mM EGTA, 20 mM *N,N*-bis-(2-hydroxyethyl)-2-aminoethanesulfonic acid (pH 7.0), 200 mM ionic strength, adjusted with sodium methane sulfonate, 1 mM dithiothreitol, and 50% glycerol) containing 0.5% Triton X-100, for 1 h at 4°C. Aluminum T-clips were used to mount the fibers on a mechanical rig (17) in relaxing solution, and the temperature was set at 15°C. The fiber was stretched until just taut and then lengthened by 1%-muscle-length increments until it reached 5% above just taut length. For sinusoidal analysis (next section), the fiber was activated to pCa 5.0 by three partial solution exchanges with activating solution. Sinusoidal analysis was performed in activating solution. The fiber was stretched by 2%-muscle-length increments until work output, as determined by sinusoidal analysis, was maximal (typically requiring a total stretch of 6%). Relaxing solution was then exchanged into the chamber, tension measured, and step and sinusoidal analysis repeated.

Sinusoidal analysis

Sinusoidal analysis was performed as in Dickinson et al. (17). Briefly, sinusoidal length changes of 0.25% muscle length (peak to peak) were applied over 47 frequencies, from 0.5 to 1000 Hz, to the fiber. For each frequency, the elastic and viscous moduli were calculated from the length and force transients by computing the amplitude ratio and the phase difference for force and length. The ratio was divided by fiber cross-sectional area. Work (Jm^{-3}) = $\pi E_v (\Delta L/L)^2$ and power (Wm^{-3}) = $\pi f E_v (\Delta L/L)^2$,

TABLE 1 Flight characteristics

	Flight index, 22°C	WBF (Hz), 22°C	Flight index, 15°C	WBF (Hz), 15°C
IFI	3.9 ± 0.2 (66)	180 ± 5 (10)	1.9 ± 0.2 (52)	147 ± 1.7 (11)
IFI-7a, line 37A	3.6 ± 0.4 (46)	176 ± 3 (13)	1.3 ± 0.2 (66)*	143 ± 2.6 (13)
IFI-7a, line 86A	3.8 ± 0.3 (31)	176 ± 4 (12)	1.3 ± 0.2 (68)*	141 ± 1.4 (10)[†]

All values are mean ± SE. Numbers in parentheses indicate the number of flies tested. Line 37A and line 86A are independently generated, transgenic IFI-7a lines.

*Statistically different from IFI (*t*-test, $p = 0.04$).

[†]Statistically different from IFI (*t*-test, $p = 0.02$).

where f is the frequency of the length perturbations (s^{-1}), E_v is the viscous modulus at f, A is the fiber cross-sectional area (m^2), and $\Delta L/L$ is the amplitude of the sinusoidal length change divided by the length of the fiber between the two T-clips.

Step analysis

To determine the rate of tension redevelopment (r_3), activated fibers were subjected to a series of four identical 0.5% muscle-lengthening steps (9). The force response was averaged over the four steps. The force response was fit to the sum of three exponential curves: $a_1(1 - \exp(-k_1 t)) + a_2\exp(-k_2 t) + a_3\exp(-k_3 t) + $ offset. Constants a_1, a_2, and a_3 are amplitudes; k_1, k_2, and k_3 are rate constants; and k_1 is r_3. The offset adjusts for nonzero starting values.

Flight assays

Flight ability and wing-beat frequency were measured at 22°C (room temperature) and also at 15°C (the temperature at which the muscle mechanical measurements were performed), thus allowing direct comparison of muscle kinetics and flight parameters. Wing-beat frequency of a tethered fly was determined using an optical tachometer (18). Flight ability was assayed by observing whether a fly is capable of flying up (U), horizontally (H), down (D), or not at all (N), when released in a plexiglas flight chamber (19). Flight index equals $6\,U/T + 4\,H/T + 2\,D/T + 0\,N/T$, where T is the total number of flies tested (20).

Ultrastructural integrity of myofibrils expressing chimeric myosins

Previously, we found no difference in the ultrastructural properties, e.g., hexagonal packing of thick and thin filaments, of the IFI and IFI-7a myofibrils at 2 days and 1 week of age when viewed longitudinally and cross-sectionally by transmission electron microscopy (16).

EMB-7d myofibrillar assembly is indistinguishable from wild-type myofibrils but, in contrast to IFI-7a, the sarcomeres undergo progressive degradation in a manner similar to that of IFM fibers expressing EMB myosin (16). In pupae there are no significant differences between EMB-7d and wild-type, but at 2 days post eclosion, EMB-7d and EMB both show obvious signs of degradation, e.g., disorder in filament packing. At <2 h posteclosion there are only very minor signs of degradation (16). Thus, as was the case with our previous studies of fibers expressing EMB and chimeric EMB constructs (4,9), we used fibers from flies that had just eclosed (wings still curled up) to minimize the impact of any myofibril structural degradation on mechanical properties. We previously showed that, unlike the damage that occurs during aging, no appreciable damage to EMB fibers occurs during the course of our experiments. The amount of fiber ''rundown'' during the course of the experiment was similar in mutant and wild-type controls (9), indicating any kinetic mismatch between very fast fibers and slow myosin isoforms did not adversely affect muscle performance.

Two-hour-old *Drosophila* myofibril diameter is less than that of 2-day-old myofibril diameter, as IFM development continues for at least several hours after eclosion, with additional thick and thin filament accumulation (21). The reduced number of filaments per myofibril results in lower power, tension, and work values from young fibers, as evident from our previous experiments on <2-h-old IFI control fibers (denoted IFI-2h) compared to 2-day-old IFI fibers (9). Thus all mechanical values normalized to fiber cross-sectional area are compared only to fibers of the same age. In contrast, the kinetics of IFI and IFI-2h were similar (9); thus, kinetic properties such as f_{max}, which do not depend on cross-sectional area, are directly comparable between fibers from flies of any age.

RESULTS

Flight ability

Previously, we observed that IFI-7a *Drosophila* fly as well as IFI at 22°C (16). To expand our examination of flight ability, we repeated the flight ability testing and also measured wing-beat frequency (WBF) at two temperatures. At 22°C, we found no statistically significant difference between IFI and IFI-7a for flight index or WBF (Table 1). However, at 15°C, the temperature at which we performed the fiber mechanical measurements, we saw small, but statistically significant differences in flight ability between IFI-7a and IFI flies (Table 1). Flight index was slightly lower in both IFI-7a lines tested compared to IFI ($p = 0.04$), and wing-beat frequency was significantly lower for one of the lines ($p = 0.02$) compared to IFI. There were no differences between the two IFI-7a lines for any of the flight performance measures.

Neither EMB nor EMB-7d *Drosophila* can fly at any temperature. This is not surprising because fibers from these lines are not able to generate power when oscillated at frequencies corresponding to those that support flight (see below).

Complex stiffness and phase of IFM fibers

Sinusoidal analysis revealed differences in the complex stiffness of EMB-7d compared to EMB (Fig. 2 *A* and Table 2). EMB-7d complex stiffness was higher than EMB stiffness at almost all frequencies tested. The EMB-7d phase plot was shifted to the right, indicating an increase in speed of fiber kinetics compared to EMB.

In contrast, no difference was observed between IFI-7a and IFI (Fig. 2 *B* and Table 2). IFI-7a complex stiffness amplitude was not significantly different from IFI over all frequencies tested. No difference was observed in the phase plot, suggesting no change in overall fiber kinetics.
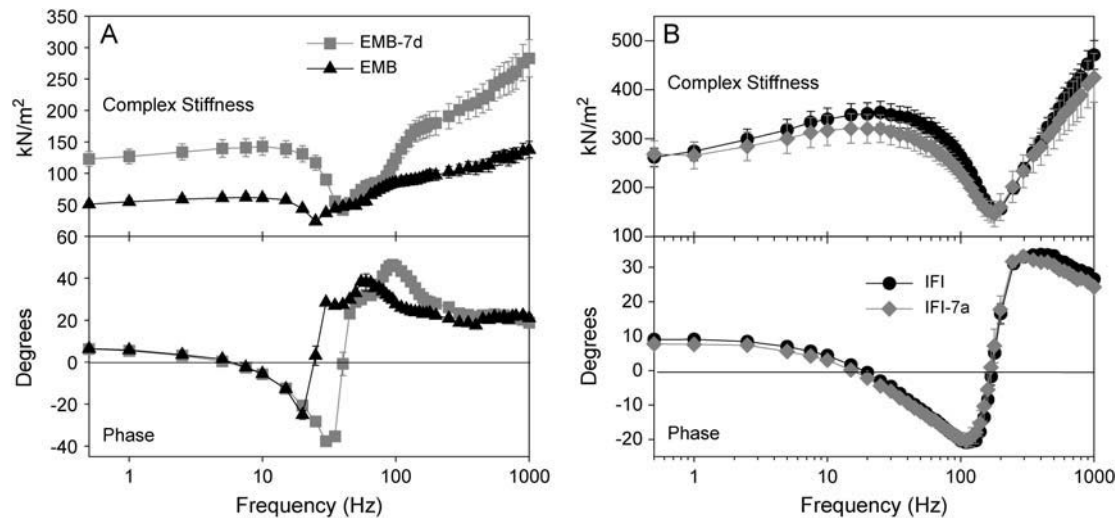
FIGURE 2 Complex stiffness and phase shift of maximally Ca^{2+}-activated IFM fibers at 15°C. (A) Complex stiffness and phase as a function of frequency for EMB-7d and EMB fibers from <2-h–old adults. (B) Complex stiffness and phase as a function of frequency for IFI and IFI-7a IFM fibers from 2-day-old flies. Note the different y axis scales for complex stiffness in A and B, as fibers from the younger flies have less myofibril area per cross section (see Methods).

Elastic and viscous moduli of IFM fibers

Separating the complex stiffness into its elastic and viscous components (Fig. 3) provides more specific information about a fiber's mechanical properties. The viscous modulus reveals information about active force-generating (negative values) or absorbing processes (positive values). The elastic modulus primarily reveals changes in passive muscle elements (connecting filaments, thin and thick filaments). For EMB-7d, we saw a rightward shift in both the elastic and viscous moduli compared to EMB (Fig. 3), suggesting that EMB-7d fibers operate best at faster oscillation speeds than EMB fibers. The EMB-7d elastic modulus was stiffer (greater) than that of EMB at most frequencies (Fig. 3 A, Table 2). Its viscous modulus dips lower (negative viscous modulus = net work produced) than that of EMB, suggesting that EMB-7b produced more work, which was confirmed by comparing the minimum viscous modulus amplitude ($-E_v$) for EMB-7d and EMB fibers (Table 2). Since muscle-length change for both fibers was identical at all frequencies, maximum work

per cycle is proportional to the viscous modulus (E_v). The greater viscous modulus of EMB-7d at higher frequencies suggests it is capable of absorbing more work than EMB (Fig. 3 A). The higher elastic modulus at almost all frequencies shows that the EMB 7d fiber is also capable of recovering more work than EMB. No statistically significant differences were observed for the elastic and viscous moduli of IFI and IFI-7a fibers (Fig. 3 B and Table 2). This indicates that substitution of exon 7a had no influence on amount of work produced, stiffness, or kinetics of work production of IFI fibers.

Power generation of IFM fibers

The most physiologically relevant mechanical measure of the flight muscle is oscillatory power. The effect of the IFI exon 7 region on EMB power was substantial. EMB-7d frequency of maximum power generation (f_{max}) was 1.5-fold greater than that of EMB, and P_{max} increased 3.2-fold at 15°C (Fig. 4, Table 2). Above 20 Hz, EMB-7d power production was much

TABLE 2 Summary of dynamic properties

	N	Complex stiffness ($kN\ m^{-2}$)	$-E_v$ ($kN\ m^{-2}$)	fE_v (Hz)	E_e ($kN\ m^{-2}$)	P_{max} ($W\ m^{-3}$)	f_{max} (Hz)	r_3 (s^{-1})
IFI	14	237 ± 13	95 ± 9	106 ± 5	219 ± 12	49 ± 4	137 ± 3	1325 ± 43
IFI-7a, line 37A	12	212 ± 24	84 ± 7	102 ± 4	197 ± 24	41 ± 3	136 ± 6	1293 ± 63
EMB	12	68 ± 5	28 ± 3	20 ± 0.4	59 ± 4	2.5 ± 0.2	20 ± 0.2	101 ± 3
EMB-7d, line F40A	12	108 ± 8[†]	71 ± 6[†]	28 ± 0.7[†]	92 ± 7[†]	8.0 ± 0.6[†]	29 ± 0.4[†]	191 ± 6[†]
EMB-7d, line M23C	6	113 ± 22[†]	72 ± 13[†]	30 ± 0.8[†]	99 ± 19[†]	8.9 ± 0.16[†]	30 ± 0.6[†]	149 ± 5[†]

Complex stiffness and elastic modulus (E_e) values for IFI and IFI-7a were measured at the frequency (f_{max}) at which IFI generated maximum power (P_{max}). E_e and complex stiffness values for EMB and EMB-7d were measured at the specific f_{max} of each fiber type. fE_v is the average frequency at which the viscous modulus amplitude was lowest. $-E_v$ is the average minimum amplitude for the viscous modulus. r_3 is the rate constant for phase 3 of force recovery after a quick lengthening step (see Methods). EMB-7d, line F40A, and EMB-7d, line M23C, are two EMB-7d lines created by independent transformation events. All values are presented as mean ± SE.
*Statistically different from IFI (t-test, $p < 0.05$).
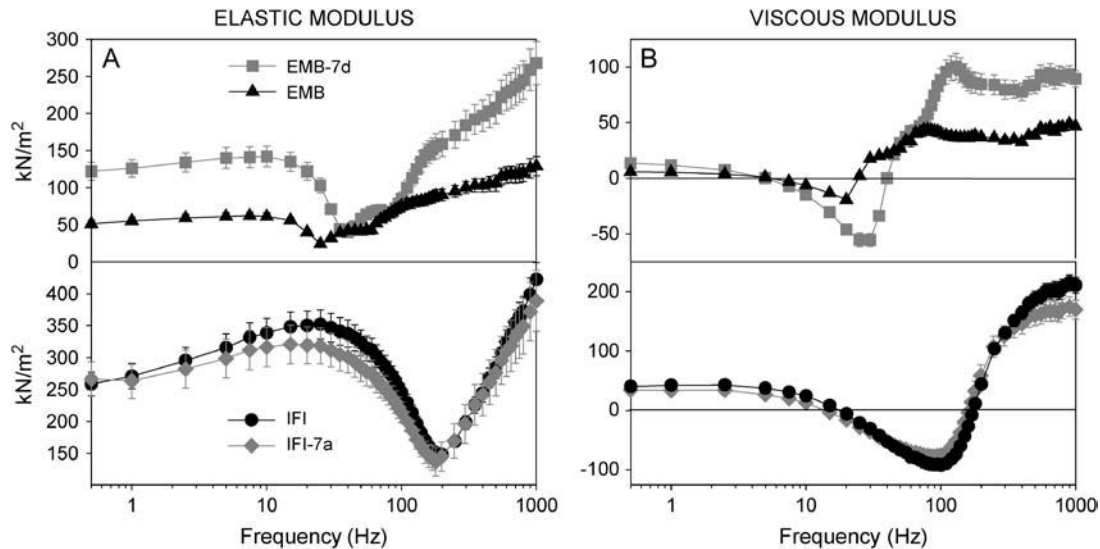[†]Statistically different from EMB (t-test, $p < 0.05$).

FIGURE 3 Elastic and viscous moduli of maximally Ca^{2+}-activated IFM fibers. (*A*) Elastic modulus (instantaneous stiffness) as a function of frequency for all four fiber types. (*B*) Viscous modulus as a function of frequency for all four fiber types.

greater than for EMB. EMB cannot generate power above 25 Hz, whereas EMB-7d generated useful power up to 40 Hz. Above 40 Hz, EMB-7d muscle was not capable of producing useful power. This frequency range is much lower than the WBF needed to support *Drosophila* flight (22).

IFI-7a maximum power (P_{max}) occurred at the same frequency as IFI, 136 Hz (f_{max}, Table 2, Fig. 4). P_{max} for IFI-

7a fibers was not statistically different from IFI (Table 2, $p = 0.19$).

Rate of force redevelopment, r_3

To confirm the differences in fiber kinetics seen with sinusoidal analysis, we employed a more traditional measure, step analysis (23,24). We measured T3 or r_3 after fitting the force response to a step increase in length (Fig. 5, Table 1). The time domain measure, r_3, should be similar to our sinusoidal frequency domain measures, e.g., f_{max}. EMB-7d r_3 was 1.9-fold faster than EMB r_3. Conversely, exchanging exon 7a into
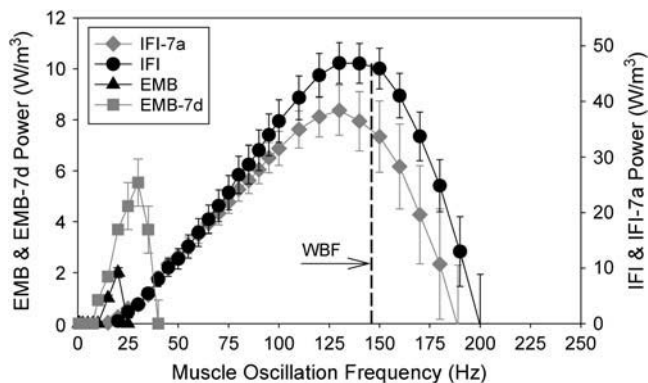

FIGURE 4 Power generation by maximally activated IFM fibers at 15°C. Power generated by EMB, EMB-7d, IFI, and IFI-7a muscle fibers when oscillated at 0.25% peak-to-peak strain over a frequency range of 0.5–250 Hz. Note the separate *y*-axis scale for EMB and EMB-7d. EMB and EMB-7d fibers generate less power than IFI and IFI-7a fibers, since these fibers are from flies <2 h-old (see text). The EMB and EMB-7d *y* axis has been scaled so that if one reads the power values from the IFI *y* axis this would be approximately the amount of power generated by EMB and EMB-IR fibers if they were the same age as 2-day-old IFI and IFI-ER fibers. The scaling is based on a previous comparison of <2-h-old fibers from EMB and IFI flies (9). WBF of IFI flies (Table 1) is indicated (*vertical dashed line*) at the corresponding muscle oscillation frequency. EMB and EMB-7d fibers cannot generate power over the normal range of wing-beat frequencies that support flight.
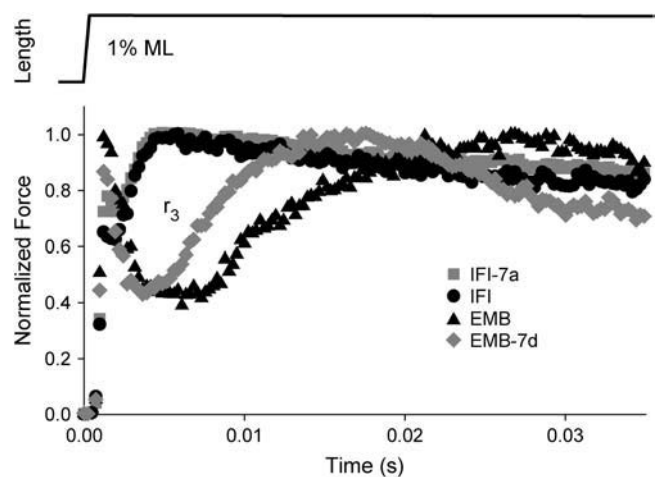

FIGURE 5 Rates of tension redevelopment (r_3). IFM fibers at pCa 5.0 were subjected to a rapid lengthening step, 0.5% muscle length. Representative traces of IFI-7a, IFI, EMB, and EMB-7d are shown with tension levels normalized to maximum tension following phase 3.

IFI resulted in no difference in r_3 compared to IFI. Thus, the r_3 values closely paralleled the differences, or lack of differences, in f_{max} and f_{Ev} measured from sinusoidal analysis (Table 1).

Isometric tension

The exon 7 region does not appear to significantly influence isometric tension (Table 3), suggesting that this region is not responsible for the marked difference in EMB and IFI isometric tensions reported previously (4). Although isometric tension tended to be higher in IFI-7a and EMB-7d than in IFI and EMB, respectively, the values were not statistically different.

DISCUSSION

Influence of the exon 7 region on fiber mechanical properties

This study furthers our understanding of regions of myosin that set muscle fiber type properties. Our analysis of two of the four exon 7 alternative versions demonstrates that the exon 7 region influences muscle kinetics, although less so than the exon 3 and 11 regions (4,9). The exchange of exon 7 caused a 50% increase in EMB f_{max} (optimal fiber speed), 10% of the 7.5-fold difference in f_{max} values of IFI compared to EMB fibers. Therefore, some of the amino acid differences between 7d and 7a affect steps of the myosin cross-bridge cycle kinetics that significantly increase slow-muscle kinetics. However, exchanging exon 7a into IFI (IFI-7a) did not affect fiber kinetics; thus it is likely that the amino acids changed by this opposite substitution are not critical for very-high-speed muscle kinetics.

Neither the 7d nor 7a substitution altered an obvious difference between IFI and EMB, an extra kinetic process seen in the EMB viscous modulus Bode plot at 50–100 Hz (Fig. 3 B). In this region of positive viscous modulus, fibers absorb work. The difference in work absorption is not related to an age difference between the 2- to 3-day IFI fibers and the 2-h EMB fibers. As previously shown, IFI-2h Nyquist plots have identical shapes to those of the older IFI. We interpret the ''bump'' as an extra kinetic ''process'' (9), which most

TABLE 3   Isometric properties

	Number	T_{max} (mN/mm^2)	Passive tension (mN/mm^2)
IFI	14	0.73 ± 0.09	0.89 ± 0.12
IFI-7a, line 37A	12	0.88 ± 0.17	0.96 ± 0.11
EMB	12	0.49 ± 0.07	0.46 ± 0.04
EMB-7d, line F40A	12	0.63 ± 0.09	0.54 ± 0.04
EMB-7d, line M23C	6	0.73 ± 0.14	0.61 ± 0.12

T_{max} and passive tension values for IFI-7a were not statistically different from those of IFI, and values for EMB-7d lines were not different from those for EMB ($p > 0.05$, t-test). T_{max}, net active tension (gross active tension minus passive tension). All values are presented as mean ± SE.

likely represents a rapid myosin isomerization that changes the stiffness of the cross-bridge, or a fast transition between different-strength actin-binding states. IFI either lacks this process, or it occurs at a higher frequency than we are sampling. Since exon 7d did not eliminate this process (80–120 Hz for EMB-7d in Fig. 3 B) from EMB and 7a did not confer it to IFI, we conclude that exon 7 is not responsible for this process.

Correlations between fiber kinetics and actomyosin ATPase

The results of our current mechanics experiments combined with previous solution actin-activated ATPase and in vitro motility velocity data suggest that the EMB-7d exchange affects the lifetime of at least two states of the cross-bridge cycle (Fig. 6), whereas the IFI-7a exchange probably affects the lifetime of only one. The IFI-7a exchange increased ATPase ~30%, with no effect on in vitro motility velocity or fiber kinetics. A simple explanation is that the exchange only affects lifetimes of detached or weakly bound states (states _1–3_, Fig. 6), i.e., states that only influence ATPase rates. The exchange apparently did not affect any strongly bound states (states _4–8_, Fig. 6) whose durations influence in vitro motility velocity, oscillatory power, and force generation. Oxygen exchange studies of _Lethocerus_ IFM suggest that one of the steps from ATP hydrolysis to Pi release is the ATPase rate-limiting step for IFM (25). Our mechanics data suggest that the actin-activated ATPase rate-limiting step for IFM must occur before force generation, because the higher ATPase rates did not alter frequency of maximum work or power. As previous studies on fibers suggest that at least some force generation occurs before Pi release in a two-step process (26,27), we conclude that the rate-limiting step for IFM actin-activated ATPase must either be ATP hydrolysis (between states _1_ and _2_) or initial actin binding (between states _2_ and _3_) (Fig. 6).

Compelling evidence from our _Drosophila_ myosin exon 11 exchange studies (28) and other work (29,30) suggests
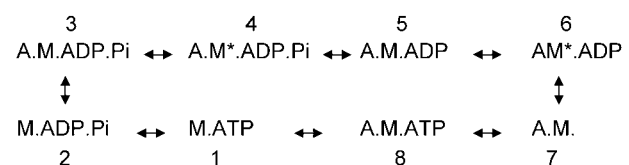

FIGURE 6   Six-state actomyosin cross-bridge model. States 1–3 are detached or weakly bound and states 4-8 are strongly bound. Because insect IFM ATPase rates (~5/s) (31) are much slower than kinetics of work production (e.g., 150 Hz for _Drosophila_) (4), the ATPase rate-limiting step must be independent of the rate-limiting step for work production. Since work production is limited by a transition between strongly bound states (states _4–8_), the ATPase rate-limiting step must be a detached state; otherwise, optimal work production rate would be limited by ATPase rate. _A_, actin; _M_, myosin; *, isomerization of actomyosin to generate a distinct state not involving product release or substrate binding.

that structural changes in myosin can influence ATPase and velocity independently and that the two properties do not have to be strongly coupled. "Uncoupling" is probably the norm for insect flight muscle. Molloy et. al. (31), for example, found that active-fiber ATPase rates are similar for different insect flight muscle types, whereas fiber kinetics (r_3) are correlated with wing-beat frequencies over a wide range (30–200 Hz). As a result of the similar ATP consumption, work per cycle must decrease with increasing insect wing-beat frequency.

In contrast, the EMB-7d exchange caused a 30% increase in ATPase rate and a 50% increase in fiber kinetics, but no change in unloaded velocity in the in vitro motility assay. Thus, in addition to affecting a detached or weakly attached lifetime, exon 7d must also influence a state of EMB myosin, the effect of which can be observed through sinusoidal length perturbation analysis (as an increase in rate of force generation) but not through the in vitro motility assay. Myosin in muscle experiences large strains, both in the direction of and opposite the direction of shortening, when undergoing forced length oscillations during sinusoidal analysis compared to those experienced in the in vitro motility assay. Thus, we hypothesize that the state influencing the rate of force generation is most likely a strongly bound state (states *4–8*, Fig. 6) that is especially sensitive to strain.

A change in the lifetime of a cross-bridge state sensitive to negative strain could account for the improved EMB-7a myofibril ultrastructure compared to EMB (16). We have previously hypothesized that the progressive EMB ultrastructure degradation with age arises because EMB myosin spends a much higher fraction of its time in strongly bound states with actin. Consequently, when muscle expressing EMB attempts to oscillate at the high frequencies required for flight, the muscle rips itself apart (4). The lengthening phase, when strongly bound myosin is negatively strained, is likely to be especially damaging. If EMB-7d myosin harbors the less deleterious negative strain characteristics of IFI myosin, EMB-7d is less likely to suffer the damage with sinusoidal oscillations seen in EMB fibers.

We found previously that the difference in isometric tension generation between EMB and IFI fibers can be accounted for, at least partially, by differences in duty ratio, i.e., the percent of total cross-bridge cycle time myosin spends bound to actin (28). Duty ratio was estimated from actin-activated ATPase V_{max} and actin sliding velocity in an in vitro motility assay. However, in the current study, the isometric tensions of fibers expressing the chimeric exon 7 myosins were not statistically different from those of their respective parent isoforms (Table 3). Thus, the shorter total cross-bridge cycle times predicted from the solution ATPase measurements are probably too small to make a significant impact on the exon 7 chimeras' duty ratios and, hence, tension levels.

The EMB-7d chimera, however, did show significantly higher active stiffness (elastic modulus) compared to EMB.

The *Drosophila* IFM is a very stiff muscle and hence a good "transducer" for measuring changes in stiffness resulting from changes in myosin properties, but it is less effective in measuring active tension, since net active tension values are similar to passive tension values (i.e., low signal/noise ratio, see Table 3). Thus, differences in duty ratio are likely to be more apparent in stiffness measurements than in isometric tension. Further, if the EMB-7d construct affects a state sensitive only to negative strain on the muscle, as postulated, then differences would only be apparent from stiffness measurements (as stiffness is measured from positive and negative oscillations of the fiber) and not from measures of isometric tension.

Molecular basis for exon 7's influence on muscle mechanical properties

The structure encoded by exon 7 forms one lip of the nucleotide-binding pocket and a portion of the adjacent external surface in the upper 50-kDa region. Thus, this region is in a favorable position to interact directly with the nucleotide in the binding pocket, and therefore to exert a kinetic effect. Specifically, a recent study with scallop S1 (32) suggests that amino acid N321 (S324 in *Drosophila* exon 7) interacts weakly with the ADP diphosphate moiety in the pre-powerstroke state versus a stronger interaction in the near-rigor state. N321's movement is the only difference in the scallop myosin nucleotide binding pocket observed between these two states. Since the rate-limiting step for ATPase occurs while myosin is in or near the pre-powerstroke state, N321's weaker interaction with the nucleotide could be important for setting ATPase kinetics. In the IFI myosin, residue 324 is an asparagine, whereas in EMB, residue 324 is a serine. Thus it is possible, even likely, that different charges at this residue could affect the strength of myosin interactions with the nucleotide.

Alternatively (or in addition), we previously suggested that the exon 7 region could influence ATPase and nucleotide kinetics by transient interactions with the loop 1 region (16). The loop 1 region, invariant in *Drosophila* myosins, is located on the opposite side of the nucleotide-binding pocket from exon 7 (16,33). Variations in the loop 1 region between slow vertebrate myosin isoforms have been shown to influence ATPase rates (34,35). If the two regions transiently interact to influence ATPase rates, it is possible that variations in exon 7 may produce effects similar to those produced by varying the loop 1 structure.

Influence of exon 7a on *Drosophila* flight ability

Although substitution of exon 7a into IFI produced no effects on flight ability at room temperature (22°C), at 15°C (the temperature at which the mechanics experiments were conducted) a slight decrease in flight performance was observed (Table 1). Generally, a reduced flight performance reflects a concomitant reduction in active fiber stiffness, since WBF

correlates with the square root of fiber stiffness (18). Although there appears to be a trend toward decreased stiffness in IFI-7a, the reduction was not significant. The reduced flight ability at 15°C may be related to a change in some other parameter that we have not yet measured in the fiber. For example, the increased ATPase rate observed in the IFI-7a solution studies may be an indicator of related changes in fiber ATPase or another energetic parameter.

Our previous study with exon 3 supports the idea that changes related to our actin-activated ATPase measurements made in solution may have more of an effect on locomotion than indicated by the mechanical measures employed in this study. Flies expressing a chimeric myosin with the EMB version of exon 3 substituted in IFI caused the largest decrease in flight parameters (especially WBF) compared to other exon exchanges (9), even though the alterations in fiber mechanics and kinetics were less than in the other exon exchanges. The IFI-3a chimera is the only instance where an alternative exon exchange has decreased solution ATPase rate. These fiber ATPase parameters may underlie aspects of locomotory changes that have yet to be accounted for.

Relative importance of alternative exons

The fiber kinetic differences between IFI and EMB attributable to the exon 7d region are only a small percentage of the overall kinetic differences between IFI and EMB, suggesting that at least one other alternative exon must play a major role in setting fiber mechanical properties. Exon 11, which encodes most of the converter region, appears to play a key role, as it has a major influence on fiber kinetics (4,28), whereas the exon 3 domain has a less pronounced influence (9). The question arises whether the combined influence of exons 3b, 11a, and 7a is enough to convert the kinetics of EMB to IFI. Independently, the IFI alternative exon versions of 11 and 3 each cause a doubling of EMB f_{max}, and exon 7 caused an ~50% increase. If the influences are additive, one would expect at least a 4.5-fold increase in f_{max} (to ~90 Hz), which is ~2/3 of the 7.5-fold difference between IFI and EMB. Thus we predict that the remaining one-third of the kinetic difference between IFI and EMB resides in the untested alternative region that comprises the relay helix, which is encoded by exon 9. Alternatively, the combined effect of exchanging exons 11, 7, and 3 is greater than the sum of the observed individual effects.

REFERENCES

1. Pette, D., and R. S. Staron. 1990. Cellular and molecular diversities of mammalian skeletal muscle fibers. *Rev. Physiol. Biochem. Pharmacol.* 116:1–76.

2. Schiaffino, S., and C. Reggiani. 1996. Molecular diversity of myofibrillar proteins: gene regulation and functional significance. *Physiol. Rev.* 76:371–423.

3. Wells, L., K. A. Edwards, and S. I. Bernstein. 1996. Myosin heavy chain isoforms regulate muscle function but not myofibril assembly. *EMBO J.* 15:4454–4459.

4. Swank, D. M., A. F. Knowles, J. A. Suggs, F. Sarsoza, A. Lee, D. W. Maughan, and S. I. Bernstein. 2002. The myosin converter domain modulates muscle performance. *Nat. Cell Biol.* 4:312–317.

5. Swank, D. M., M. L. Bartoo, A. F. Knowles, C. Iliffe, S. I. Bernstein, J. E. Molloy, and J. C. Sparrow. 2001. Alternative exon-encoded regions of *Drosophila* myosin heavy chain modulate ATPase rates and actin sliding velocity. *J. Biol. Chem.* 276:15117–15124.

6. Swank, D. M., L. Wells, W. A. Kronert, G. E. Morrill, and S. I. Bernstein. 2000. Determining structure/function relationships for sarcomeric myosin heavy chain by genetic and transgenic manipulation of *Drosophila*. *Microsc. Res. Tech.* 50:430–442.

7. Murphy, C. T., and J. A. Spudich. 2000. Variable surface loops and myosin activity: accessories to a motor. *J. Muscle Res. Cell Motil.* 21:139–151.

8. Babu, G. J., E. Loukianov, T. Loukianova, G. J. Pyne, S. Huke, G. Osol, R. B. Low, R. J. Paul, and M. Periasamy. 2001. Loss of SM-B myosin affects muscle shortening velocity and maximal force development. *Nat. Cell Biol.* 3:1025–1029.

9. Swank, D. M., W. A. Kronert, S. I. Bernstein, and D. W. Maughan. 2004. Alternative N-terminal regions of *Drosophila* myosin heavy chain tune muscle kinetics for optimal power output. *Biophys. J.* 87:1805–1814.

10. Bernstein, S. I., K. Mogami, J. J. Donady, and C. P. Emerson, Jr. 1983. *Drosophila* muscle myosin heavy chain encoded by a single gene in a cluster of muscle mutations. *Nature.* 302:393–397.

11. Rozek, C. E., and N. Davidson. 1983. *Drosophila* has one myosin heavy-chain gene with three developmentally regulated transcripts. *Cell.* 32:23–34.

12. George, E. L., M. B. Ober, and C. P. Emerson, Jr. 1989. Functional domains of the *Drosophila melanogaster* muscle myosin heavy-chain are encoded by alternatively spliced exons. *Mol. Cell. Biol.* 9:2957–2974.

13. Zhang, S., and S. I. Bernstein. 2001. Spatially and temporally regulated expression of myosin heavy chain alternative exons during *Drosophila* embryogenesis. *Mech. Dev.* 101:35–45.

14. Bernstein, S. I., and R. A. Milligan. 1997. Fine tuning a molecular motor: the location of alternative domains in the *Drosophila* myosin head. *J. Mol. Biol.* 271:1–6.

15. Hastings, G. A., and C. P. Emerson, Jr. 1991. Myosin functional domains encoded by alternative exons are expressed in specific thoracic muscles of *Drosophila*. *J. Cell Biol.* 114:263–276.

16. Miller, B. M., S. Zhang, J. A. Suggs, D. M. Swank, K. P. Littlefield, A. F. Knowles, and S. I. Bernstein. 2005. An alternative domain near the nucleotide-binding site of *Drosophila* muscle myosin affects ATPase kinetics. *J. Mol. Biol.* 353:14–25.

17. Dickinson, M. H., C. J. Hyatt, F.-O. Lehmann, J. R. Moore, M. C. Reedy, A. Simcox, R. Tohtong, J. O. Vigoreaux, H. Yamashita, and D. W. Maughan. 1997. Phosphorylation-dependent power output of transgenic flies: an integrated study. *Biophys. J.* 73:3122–3134.

18. Hyatt, C. J., and D. W. Maughan. 1994. Fourier analysis of wing beat signals: assessing the effects of genetic alterations of flight muscle structure in *Diptera*. *Biophys. J.* 67:1149–1154.

19. Drummond, D. R., M. Peckham, J. C. Sparrow, and D. C. S. White. 1990. Alteration in crossbridge kinetics caused by mutations in actin. *Nature.* 348:440–442.

20. Tohtong, R., H. Yamashita, M. Graham, J. Haeberle, A. Simcox, and D. Maughan. 1995. Impairment of muscle function caused by mutations of phosphorylation sites in myosin regulatory light chain. *Nature.* 374:650–653.

21. Reedy, M. C., and C. Beall. 1993. Ultrastructure of developing flight muscle in *Drosophila*. I. Assembly of myofibrils. *Dev. Biol.* 160:443–465.

22. Lehmann, F. O., and M. H. Dickinson. 1997. The changes in power requirements and muscle efficiency during elevated flight force production in the fruit fly, *Drosophila. J. Exp. Biol.* 200:1133–1143.

23. Ford, L. E., A. F. Huxley, and R. M. Simmons. 1977. Tension responses to sudden length change in stimulated frog muscle fibres near slack length. *J. Physiol.* 269:441–515.

24. Steiger, G. J. 1977. Stretch activation and tension transients in cardiac, skeletal and insect flight muscle. *In* Insect Flight Muscle. R. T. Tregear, editor. North Holland, Amsterdam. 221–268.

25. White, D. C., J. W. Ricigliano, and M. R. Webb. 1987. Analysis of the ATPase mechanism of myosin subfragment 1 from insect fibrillar flight muscle in the presence and absence of actin, using phosphate-water oxygen exchange measurements. *J. Muscle Res. Cell Motil.* 8: 537–540.

26. Tesi, C., F. Colomo, N. Piroddi, and C. Poggesi. 2002. Characterization of the cross-bridge force-generating step using inorganic phosphate and BDM in myofibrils from rabbit skeletal muscles. *J. Physiol.* 541:187–199.

27. Morris, C., and E. Homsher. 1998. The use of caged compounds. *In* Current Methods in Muscle Physiology: Advantages, Problems, and Limitations. H. Sugi, editor. Oxford University Press, Oxford, U.K. 71–89.

28. Littlefield, K. P., D. M. Swank, B. M. Sanchez, A. F. Knowles, D. M. Warshaw, and S. I. Bernstein. 2003. The converter domain modulates kinetic properties of *Drosophila* myosin. *Am. J. Physiol. Cell Physiol.* 284:C1031–C1038.

29. Murphy, C. T., R. S. Rock, and J. A. Spudich. 2001. A myosin II mutation uncouples ATPase activity from motility and shortens step size. *Nat. Cell Biol.* 3:311–315.

30. Sherwood, J. J., G. S. Waller, D. M. Warshaw, and S. Lowey. 2004. A point mutation in the regulatory light chain reduces the step size of skeletal muscle myosin. *Proc. Natl. Acad. Sci. USA.* 101:10973–10978.

31. Molloy, J. E., V. Kyrtatas, J. C. Sparrow, and D. C. S. White. 1987. Kinetics of flight muscles from insects with different wingbeat frequencies. *Nature.* 328:429–451.

32. Risal, D., S. Gourinath, D. M. Himmel, A. G. Szent-Gyorgyi, and C. Cohen. 2004. Myosin subfragment 1 structures reveal a partially bound nucleotide and a complex salt bridge that helps couple nucleotide and actin binding. *Proc. Natl. Acad. Sci. USA.* 101:8930–8935.

33. Pereira, J. S., D. Pavlov, M. Nili, M. Greaser, E. Homsher, and R. L. Moss. 2001. Kinetic differences in cardiac myosins with identical loop 1 sequences. *J. Biol. Chem.* 276:4409–4415.

34. Rovner, A. S., Y. Freyzon, and K. M. Trybus. 1997. An insert in the motor domain determines the functional properties of expressed smooth muscle myosin isoforms. *J. Muscle Res. Cell Motil.* 18: 103–110.

35. Sweeney, H. L., S. S. Rosenfeld, F. Brown, L. Faust, J. Smith, J. Xing, L. A. Stein, and J. R. Sellers. 1998. Kinetic tuning of myosin via a flexible loop adjacent to the nucleotide binding pocket. *J. Biol. Chem.* 273:6262–6270.